HAWC
High Altitude Water Cherenkov
Gamma-Ray Observatory

Pulsars as astrophysical TeV gamma-ray sources

Alberto Carramiñana[1] & César Álvarez[2]

[1] Instituto Nacional de Astrofísica, Óptica y Electrónica
Luis Enrique Erro 1, Tonantzintla, Puebla, México
[2] Universidad Autónoma de Chiapas

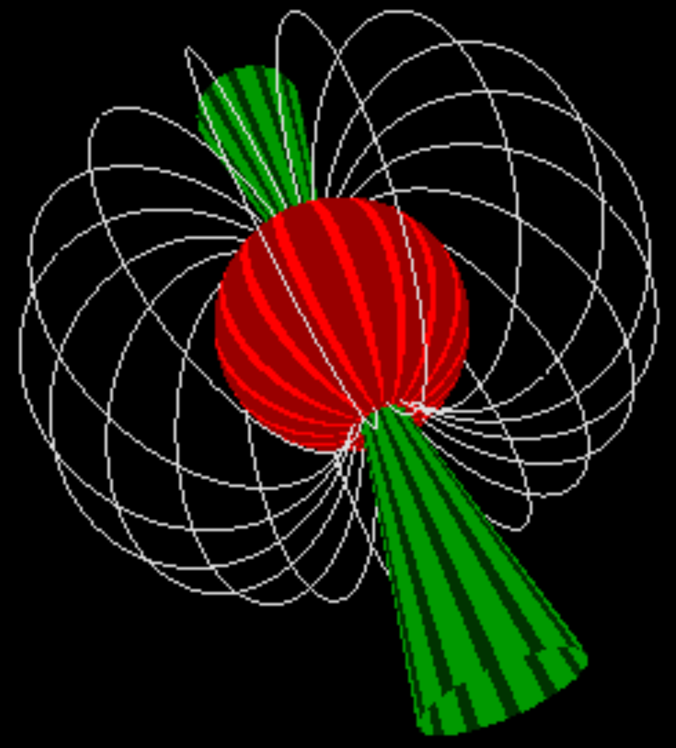

x

OAGH 2m

Reunión Anual de la División de Rayos Cósmicos SMF
En línea 23 de noviembre de 2020

INAOE

CONACYT
Consejo Nacional de Ciencia y Tecnología

This talk

- Over sixty years ago, Enrico Fermi proposed supernovae as sources of Galactic cosmic rays.
- TeV γ-ray observations show that high-energy phenomena are related to the history of high-mass stars: formation, explosion, remnants.
- Pulsars are the main type of GeV γ-ray emitters. They may be also the power engines of most Galactic TeV emitters.
  - Evolutionary scheme: PWN $\rightarrow$ TeV haloes.
- Understanding pulsar related TeV sources requires understanding of pulsar evolution and the evolution of its environment.

The Fermi paradigm

- In 1949 Enrico Fermi used magnetic mirror to show that shocks can produce power-law spectra of high-energy particles.
- Around 1954 Fermi and others argued that supernovae are particularly efficient (more than molecular clouds) and their rate is well above the energetic requirements.

$$u_{cr} \approx 0.03 \left(\frac{E_{sn}/t_{sn}}{V_{gal}} \right) t_{esc}$$

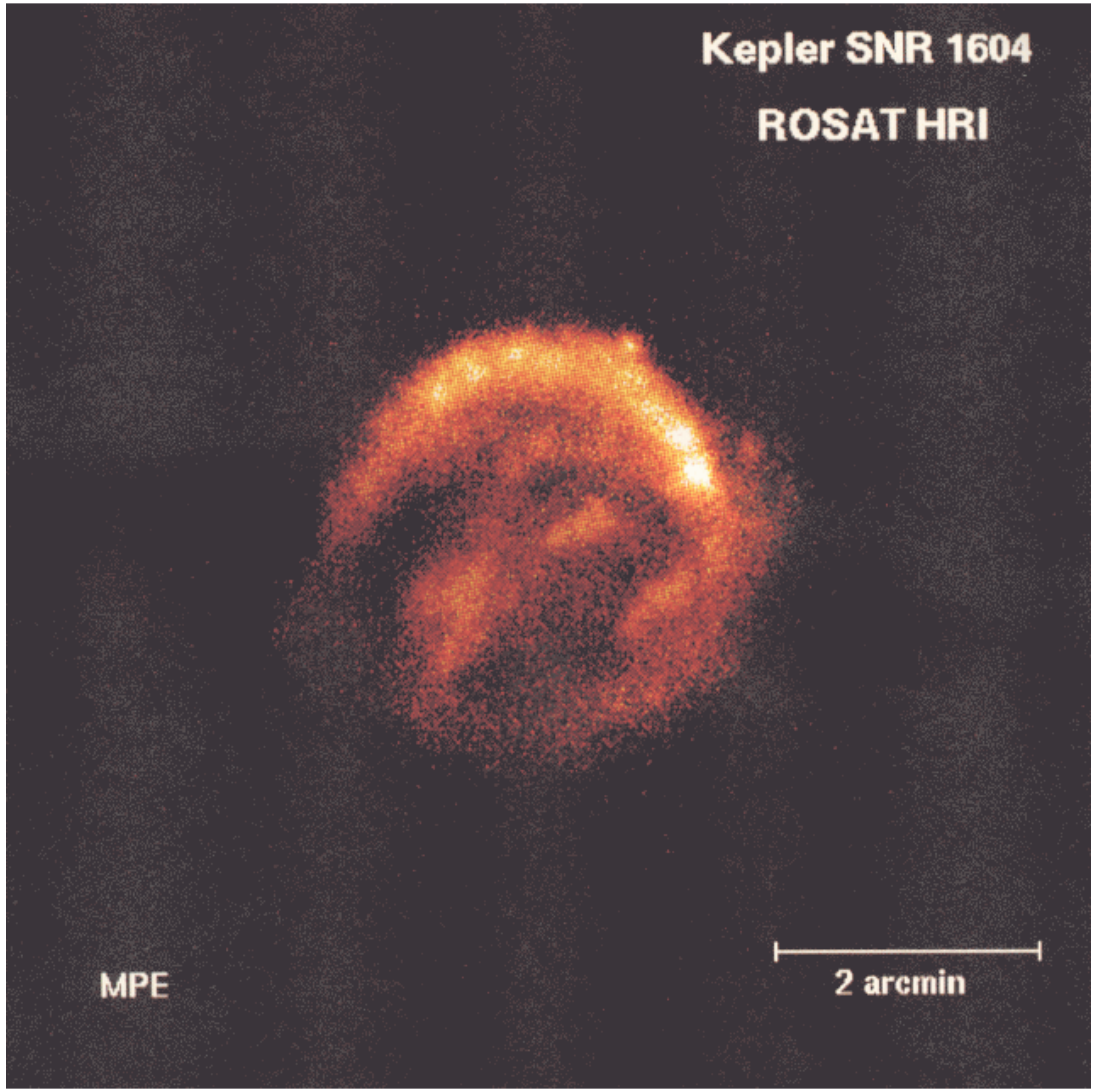

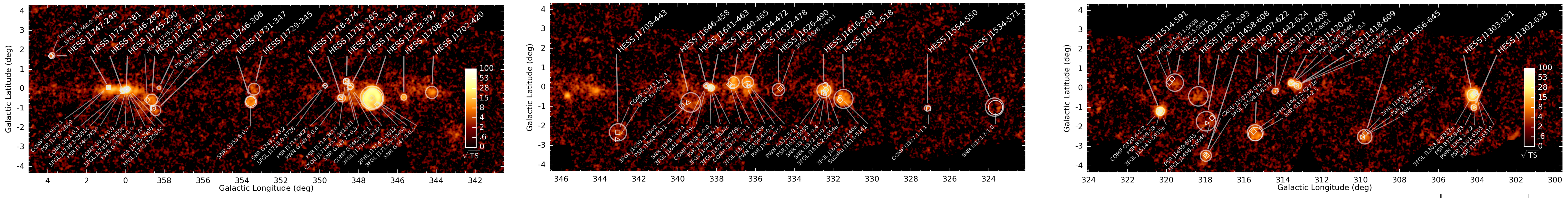

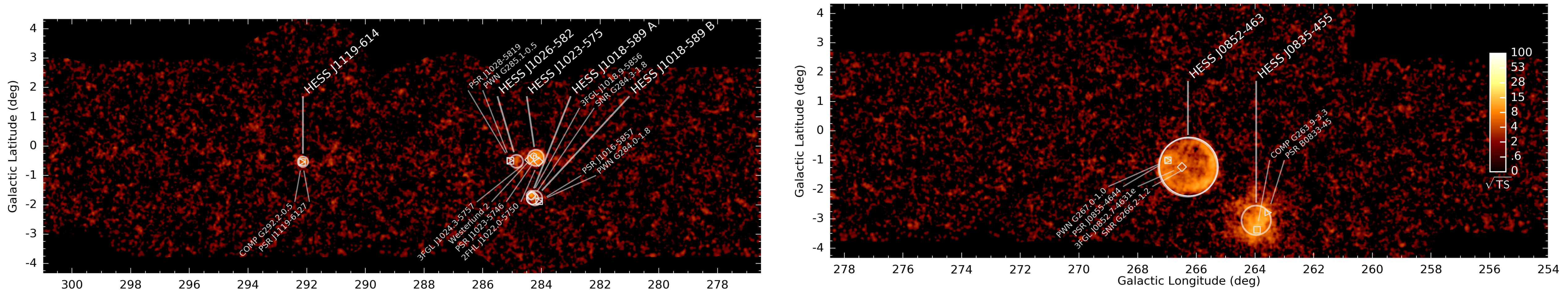

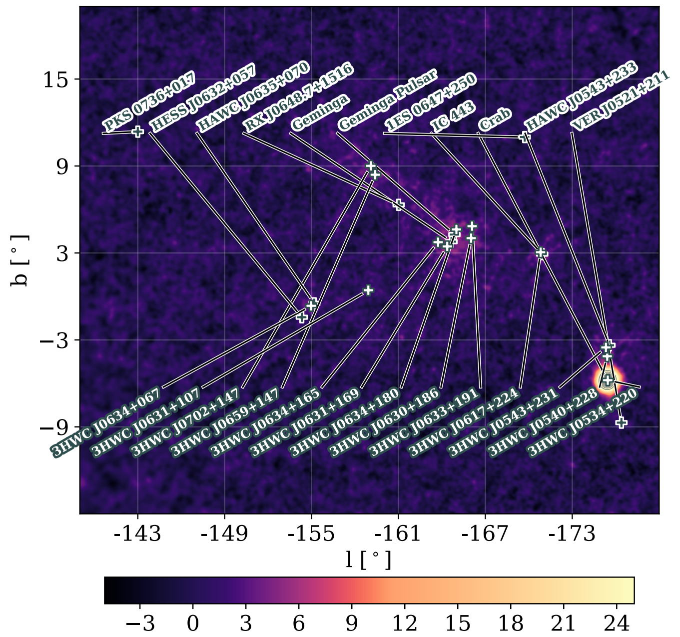

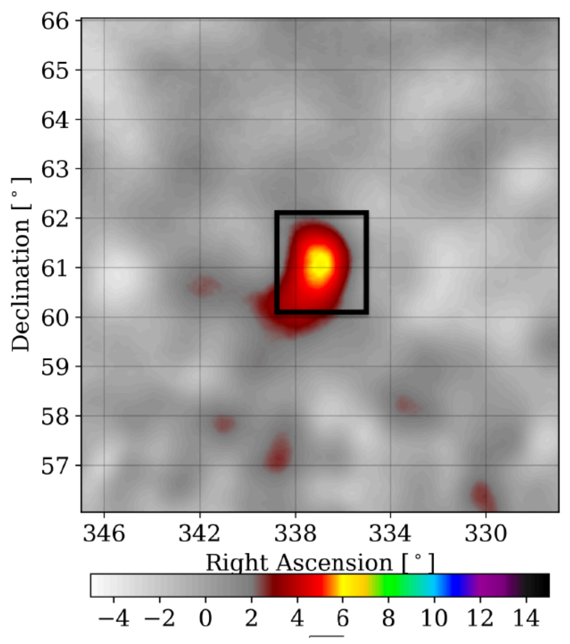

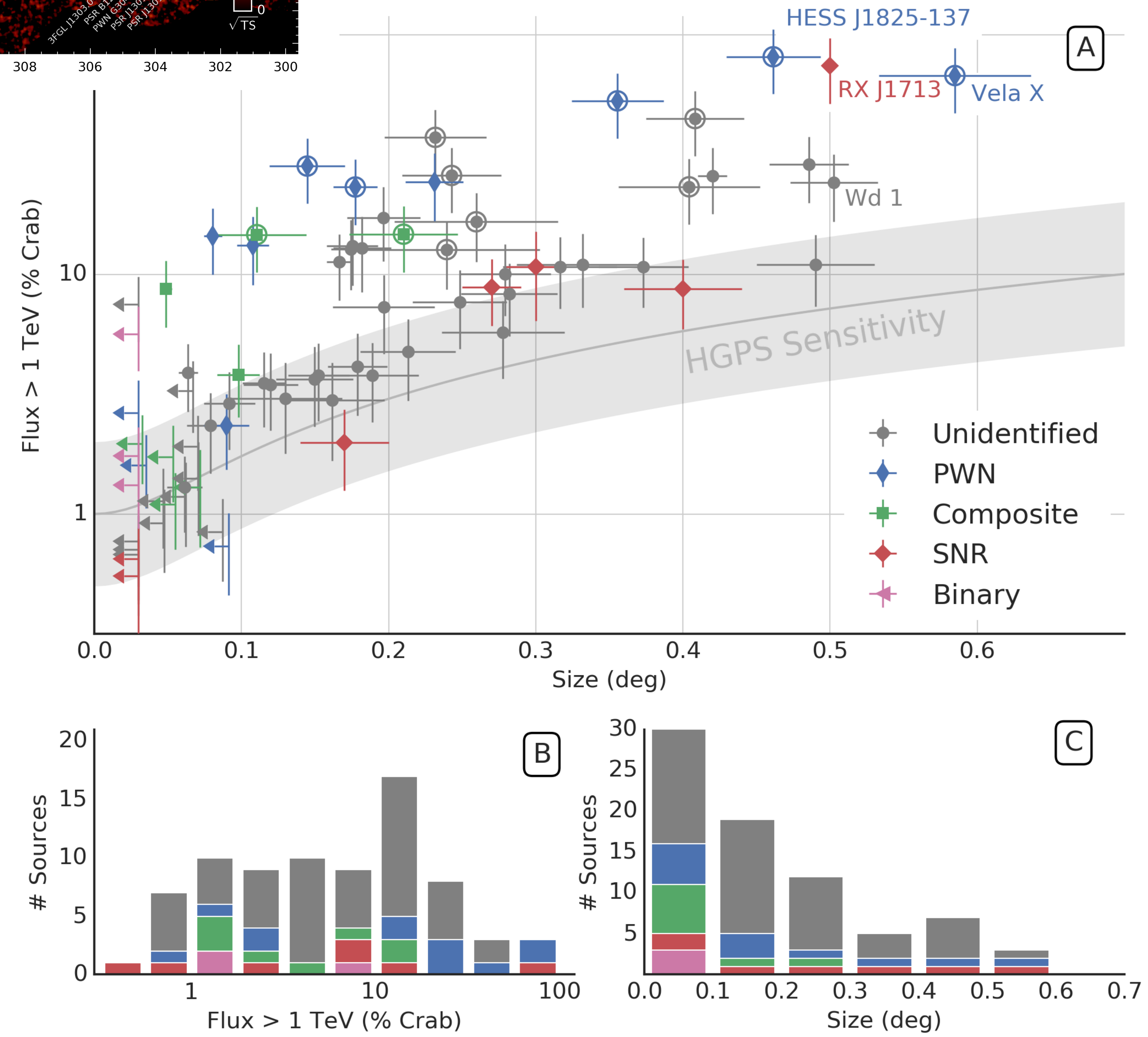

- Supernova remnants
- Pulsar wind nebulae
- Star formation regions
- Binaries incl. microquasars

High mass star formation and evolution

Galactic anticenter

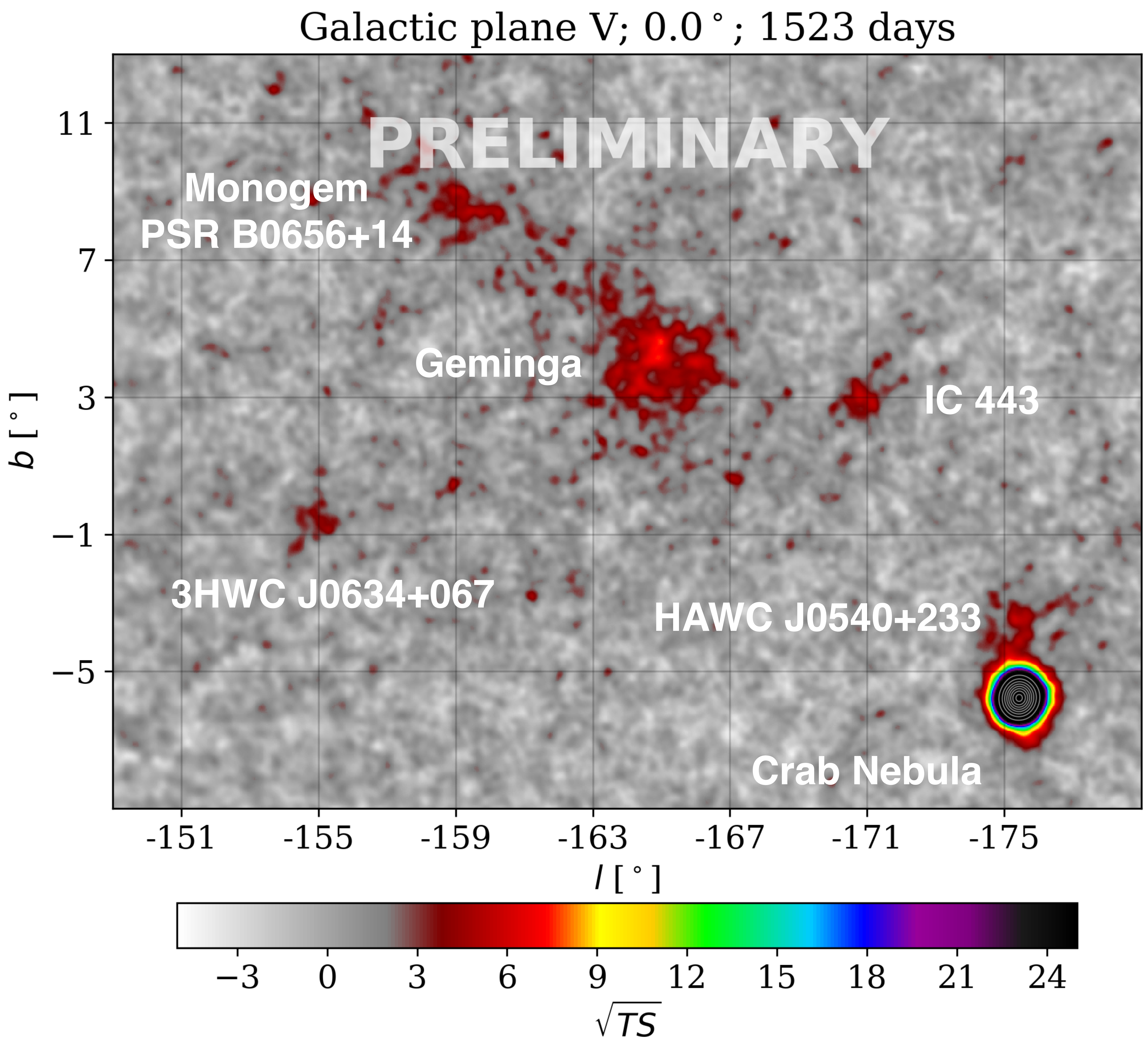

- A good sample of Galactic accelerators:
  - Crab Nebula: a prototypical Pulsar Wind Nebula (PWN).
  - Geminga & Monogem (PSR B0656+14): TeV halos
  - HAWC J0540+233 (PSR B0540+23) y 3HWC J0634+067 (PSR J0633+0632): also TeV halos?
- IC 443: classical supernova remnant.

Sudoh, Linden & Beacom: "TeV halos are everywhere"
Phys Rew D, 100, 043016 - arxiv 1902.08203

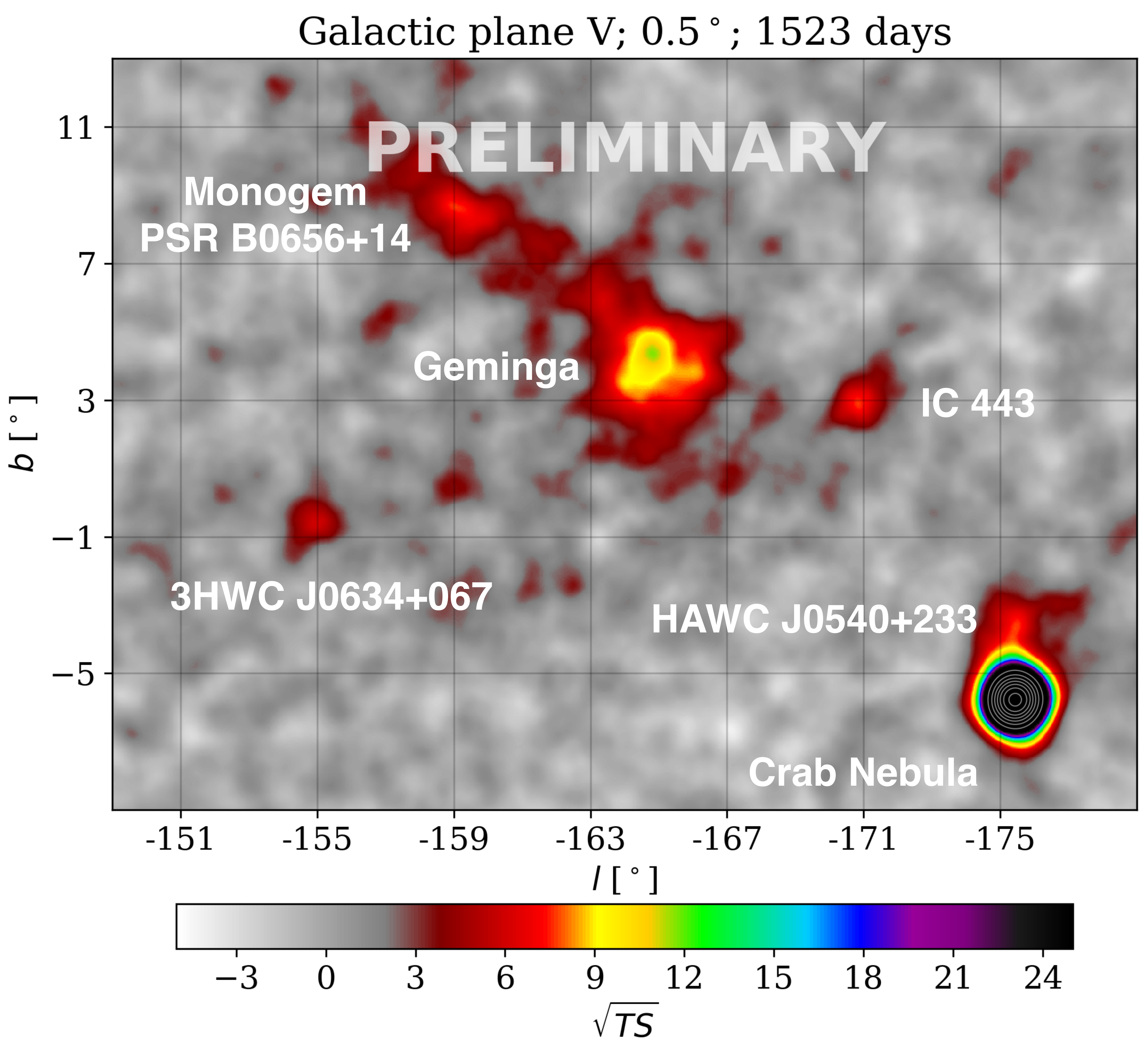

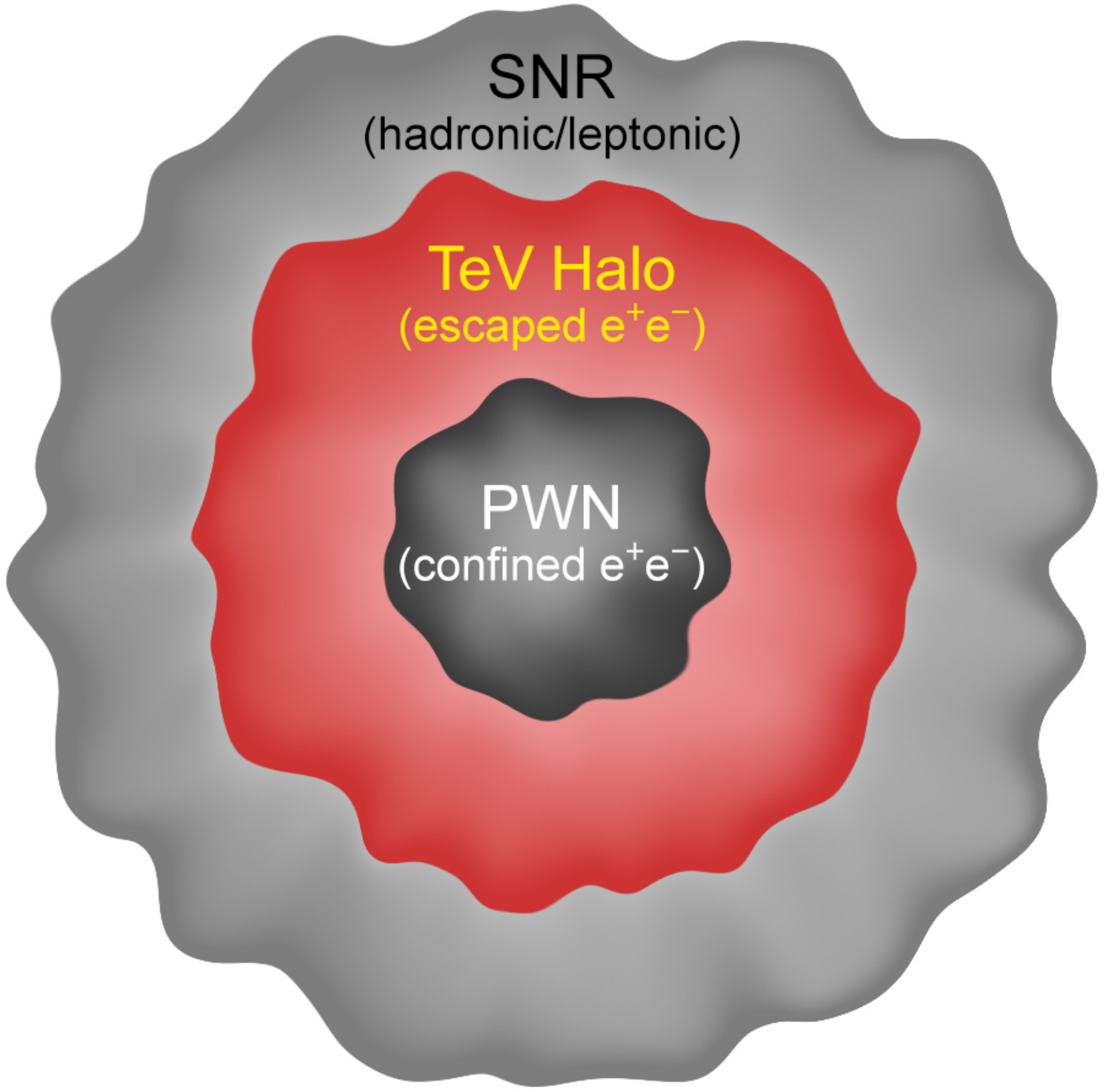

The pulsar wind pushes its environment and a TeV halo is formed. Emission is due to very energetic leptons (ICS).

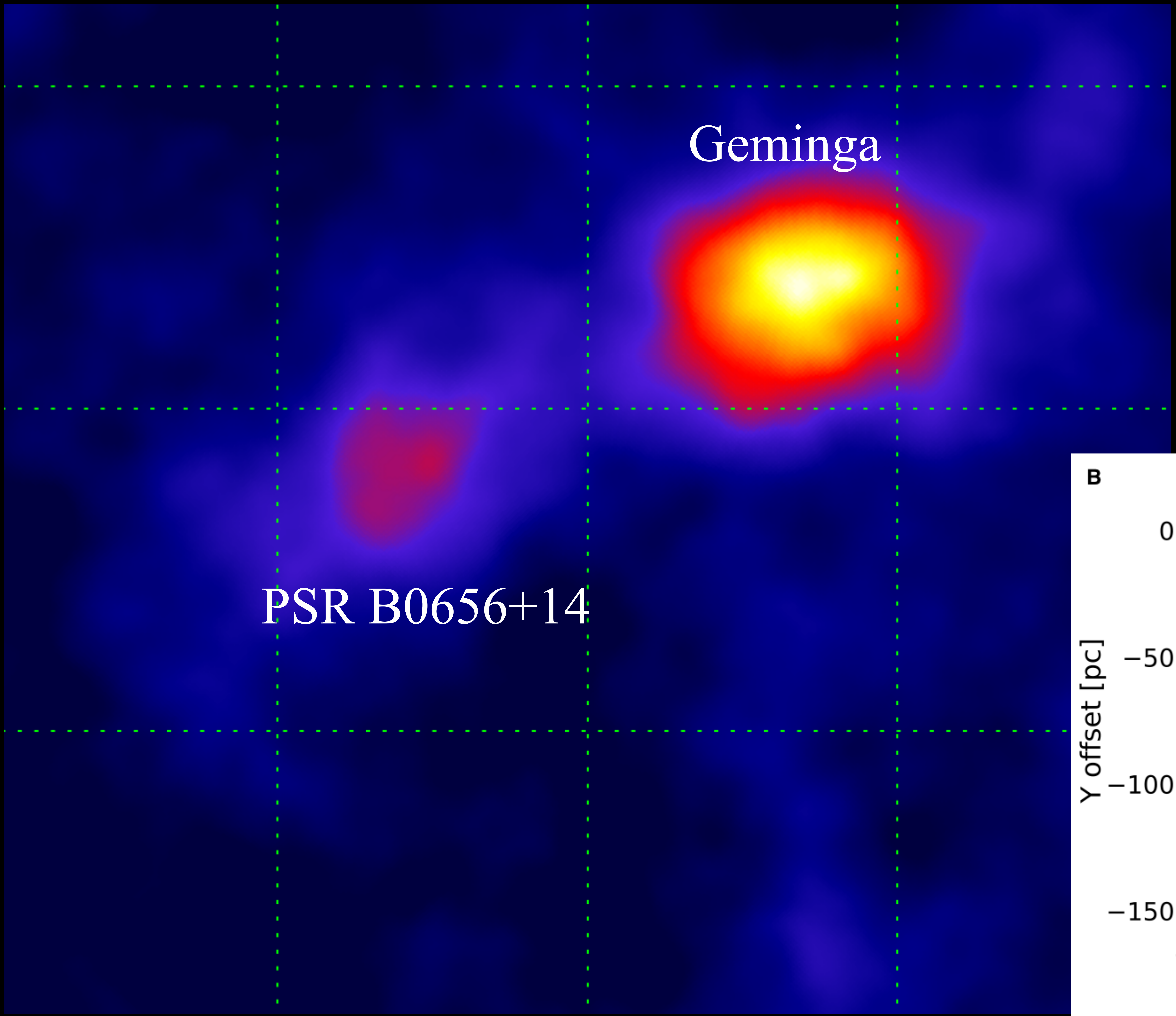
Geminga
PSR B0656+14

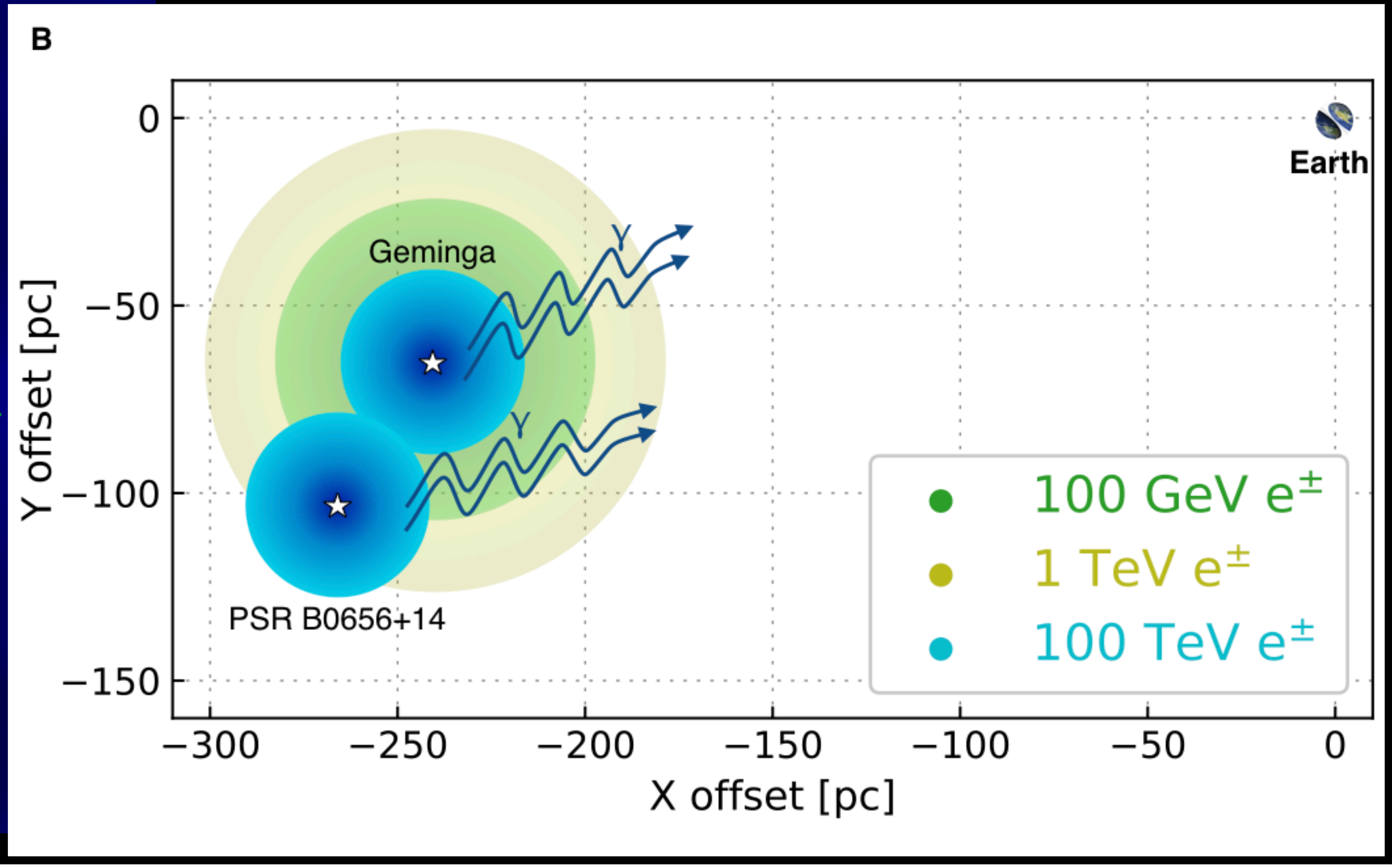
B
Geminga
PSR B0656+14
Earth
γ
Y offset [pc]
X offset [pc]
0
−50
−100
−150
−300
−250
−200
−150
−100
−50
0
100 GeV e±
1 TeV e±
100 TeV e±


PRELIMINARY
PRELIMINARY
eHWC J2030+412
eHWC J2019+368
eHWC J1907+063
eHWC J1850+001
eHWC J1842-035
eHWC J1839-057
eHWC J1825-134
HAWC J1813-176
eHWC J1809-193
E > 56 TeV
E > 100 TeV
E > 177 TeV
$\sqrt{TS}$

Extreme sources

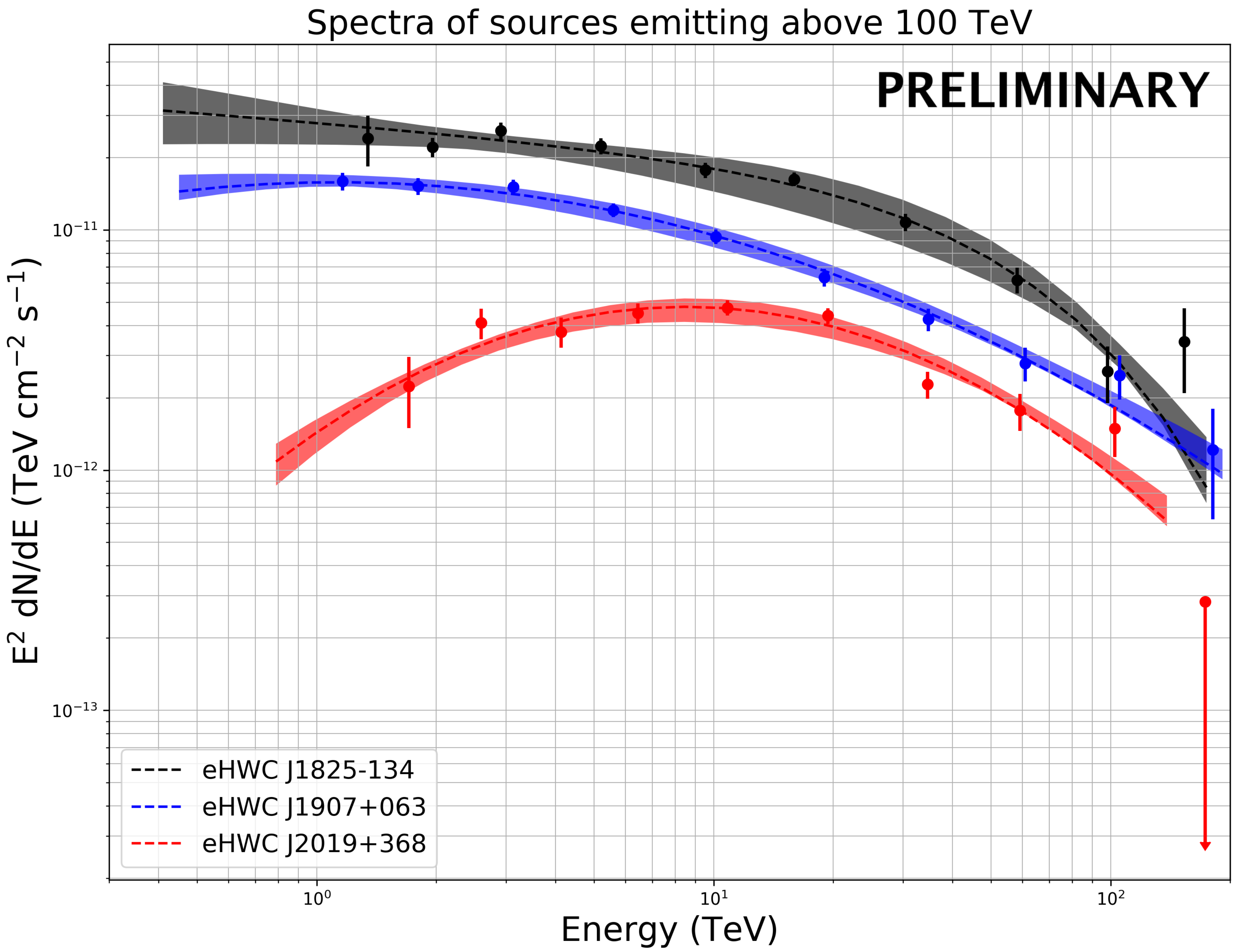

Source	p-Value	E_c (95%)	E_c (3σ)
eHWC J1825-134	1.000	244 TeV	158 TeV
eHWC J1907+063	0.990	218 TeV	162 TeV
eHWC J0534+220 (Crab Nebula)	1.000	152 TeV	104 TeV
eHWC J2019+368	0.828	120 TeV	88 TeV

Abeysekara et al. 2020, PRL 124, 021102.

TABLE III. Information on all pulsars with $\dot{E} > 10^{36}$ erg/s within 0.5° of each source. The only pulsar within 0.5° of eHWC J2030 + 412 has an $\dot{E}$ below this threshold; it is included here for completeness. All pulsar parameters come from the ATNF database, version 1.60 [34] unless specified. The distance between the pulsar and the HAWC source, as well as the HAWC high-energy source extent (from Table I), is given in parsecs here, assuming that the HAWC source is the same distance from the Earth as the pulsar.

HAWC source	PSR name	$\dot{E}$ (erg/s)	Age ($P/2\dot{P}$) (kyr)	Distance to Earth (kpc)	Distance between HAWC source and PSR [° (pc)]	HAWC source extent (pc)
eHWC J0534 + 220	J0534 + 2200	4.5×10^{38}	1.3	2.00	0.03 (1.05)	...
eHWC J1809 − 193	J1809 − 1917	1.8×10^{36}	51.3	3.27	0.05 (2.86)	19.4
...	J1811 − 1925	6.4×10^{36}	23.3	5.00	0.40 (34.9)	29.7
eHWC J1825 − 134	J1826 − 1334	2.8×10^{36}	21.4	3.61	0.26 (16.4)	22.1
...	J1826 − 1256	3.6×10^{36}	14.4	1.55	0.45 (12.2)	9.47
eHWC J1839 − 057	J1838 − 0537	6.0×10^{36}	4.89	2.0 [a]	0.10 (3.50)	11.9
eHWC J1842 − 035	J1844 − 0346	4.2×10^{36}	11.6	2.40 [b]	0.49 (20.5)	16.3
eHWC J1850 + 001	J1849 − 0001	9.8×10^{36}	42.9	7.00 [c]	0.37 (45.2)	45.2
eHWC J1907 + 063	J1907 + 0602	2.8×10^{36}	19.5	2.37	0.29 (12.0)	21.5
eHWC J2019 + 368	J2021 + 3651	3.4×10^{36}	17.2	1.80	0.27 (8.48)	6.28
eHWC J2030 + 412	J2032 + 4127	1.5×10^{35}	201	1.33	0.33 (7.66)	4.18

[a] Pseudodistance from [38].
[b] Pseudodistance from Eq. (3) of [39].
[c] Distance estimate from [40].

Abeysekara et al. 2020, PRL 124, 021102.

Pulsars

- Pulsars are the “inner remnant” of supernovae (discovered too late for Enrico Fermi).
- Pulsars were discovered in the radio band (1967) and were the first identified type of γ-ray sources, in the MeV range (Kniffen et al. 1974, Fichtel et al. 1975).
- Dominant type of Galactic source at 1 GeV (231+10 in 4FGL):
  - pulsed emission tends to break between 1 and 10 GeV.

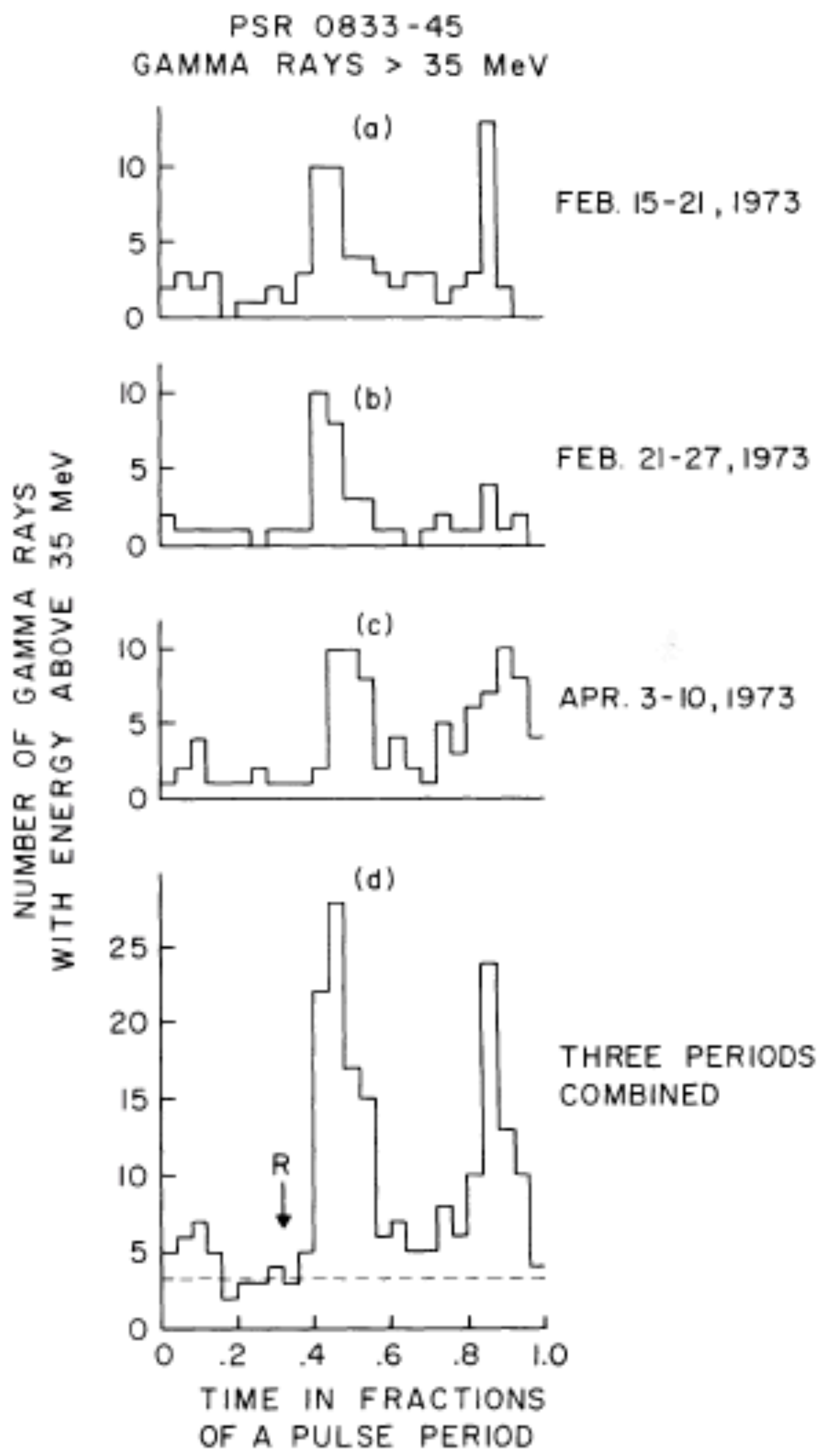

FIG. 1.—Distribution of γ-ray arrival times in fractions of a radio pulse period for γ-rays above 35 MeV from the direction of PSR 0833−45. (a) Data acquired 1973 February 14–21; (b) data acquired 1973 February 21–28; (c) data acquired 1973 April 3–10; (d) data from all three periods combined. Arrow *R* marks the position of the 2388 MHZ radio pulse (Reichley 1975). The dashed line shows diffuse radiation if n

Thompson et al. (1975)

THE ASTROPHYSICAL JOURNAL SUPPLEMENT SERIES, 208:17 (59pp), 2013 Octo

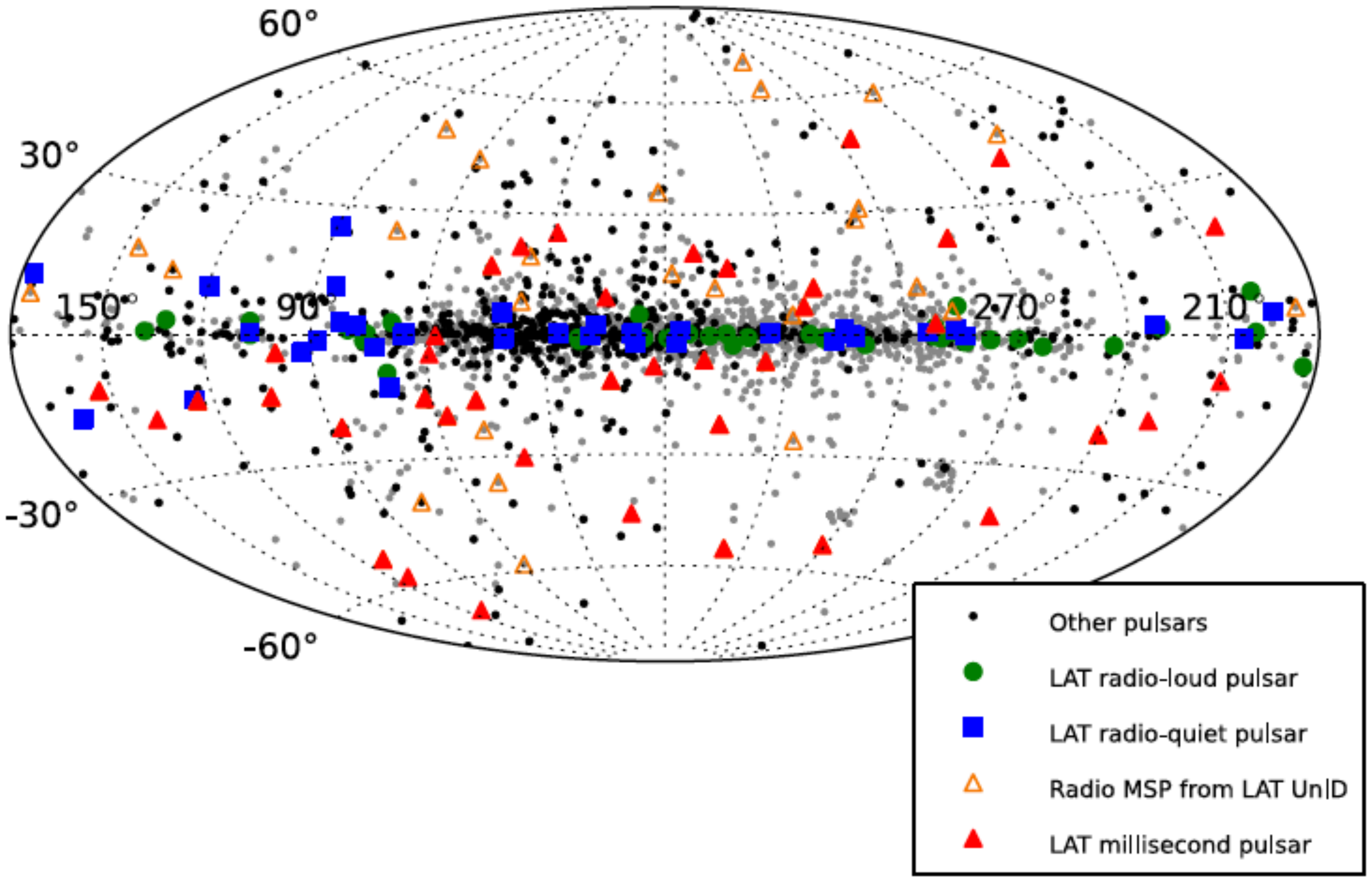

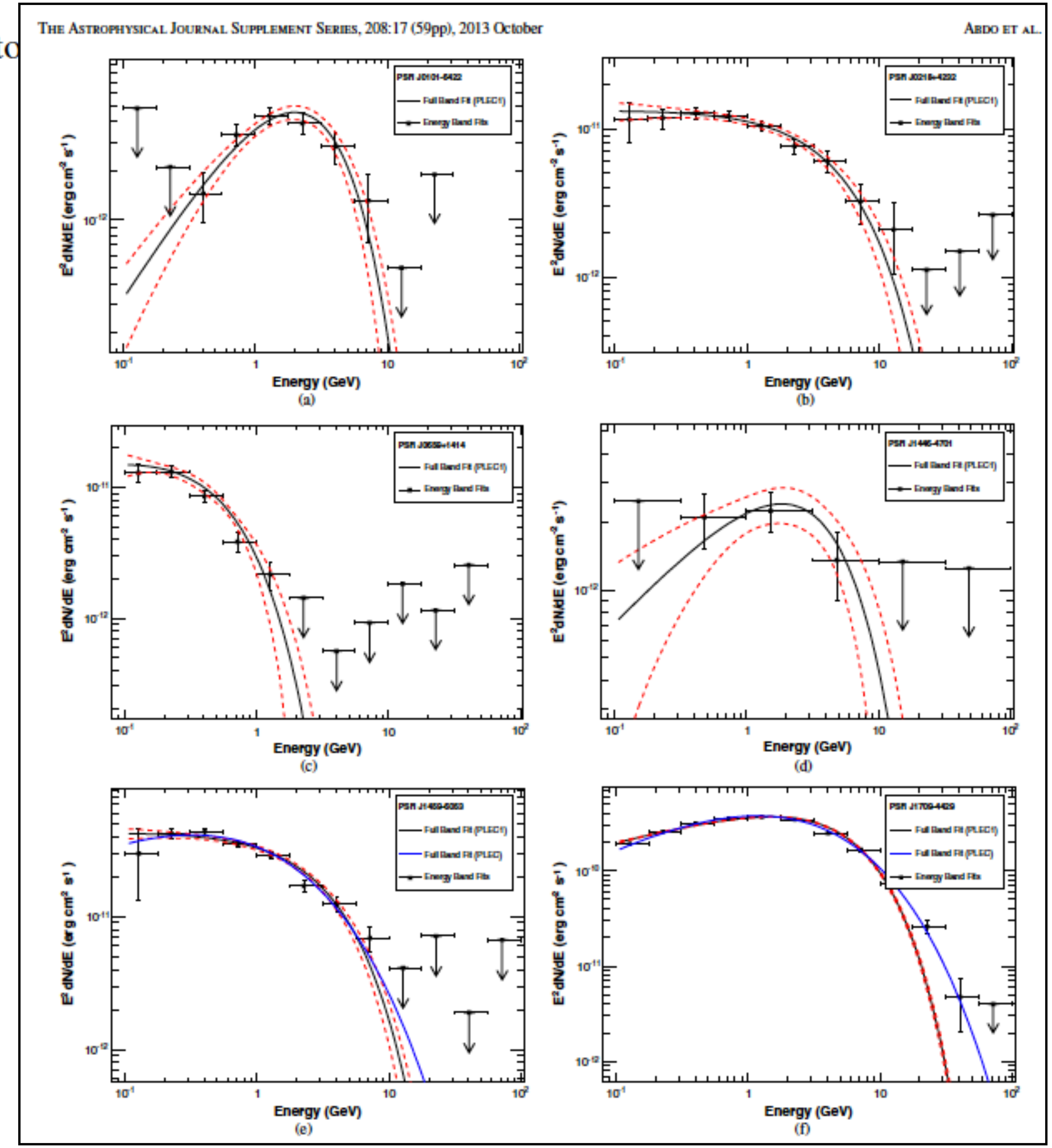

- Pulsar properties are usually described through the magnetic dipole model:
  - energetics: energy losses, magnetic field, acceleration, age and evolution

Pulsar dipole model

- Pulsar properties are usually described through the magnetic dipole model.
- Rotational energy losses due to magnetic dipole emission

$$\frac{d}{dt}\left(\frac{1}{2}I\Omega^2\right) = -\frac{2\ddot{\mu}^2}{3c^3}$$

- Energy losses, dynamical age, stellar magnetic field

$$\Rightarrow \quad \dot{E}_{rot} = 4\pi^2 I\left(\dot{P}/P^3\right) \simeq 3.9\times10^{36}\,\mathrm{erg\,s^{-1}}\,I_{45}\left[\frac{\dot{P}/10^{-13}}{(P/0.1\,\mathrm{s})^3}\right]$$

$$\Rightarrow \quad t_d = P/2\dot{P} \simeq 15\,800\,\mathrm{years}\left[\frac{P/0.1\,\mathrm{s}}{\dot{P}/10^{-13}}\right]$$

$$\Rightarrow \quad B_\star = \frac{1}{2\pi R_\star^3}\left(\frac{3}{2}Ic^3\,P\dot{P}\right)^{1/2} \simeq 3\times10^{12}\,\mathrm{G}\left(\frac{P}{0.1\,\mathrm{s}}\,\frac{\dot{P}}{10^{-13}}\right)^{1/2}$$

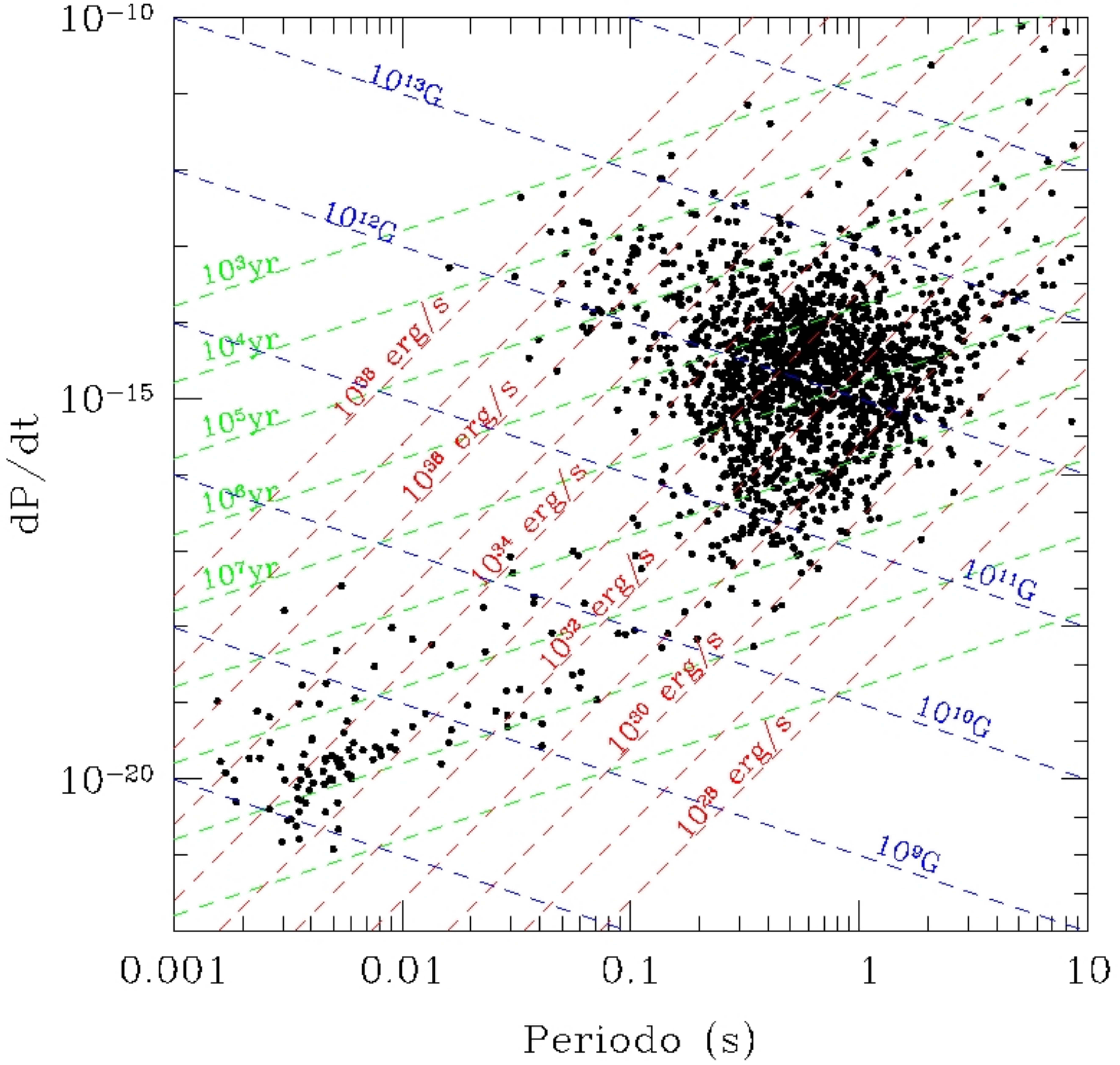

Diagrama P-dot{P}

$$\dot{E}_{rot} = 4\pi^2 I \left(\frac{\dot{P}}{P^3}\right)$$

$$t_d = \frac{P}{2\dot{P}}$$

$$B_\star = \frac{1}{2\pi R_\star^3}\left(\frac{3}{2} I c^3\, P\dot{P}\right)^{1/2}$$

Particle acceleration

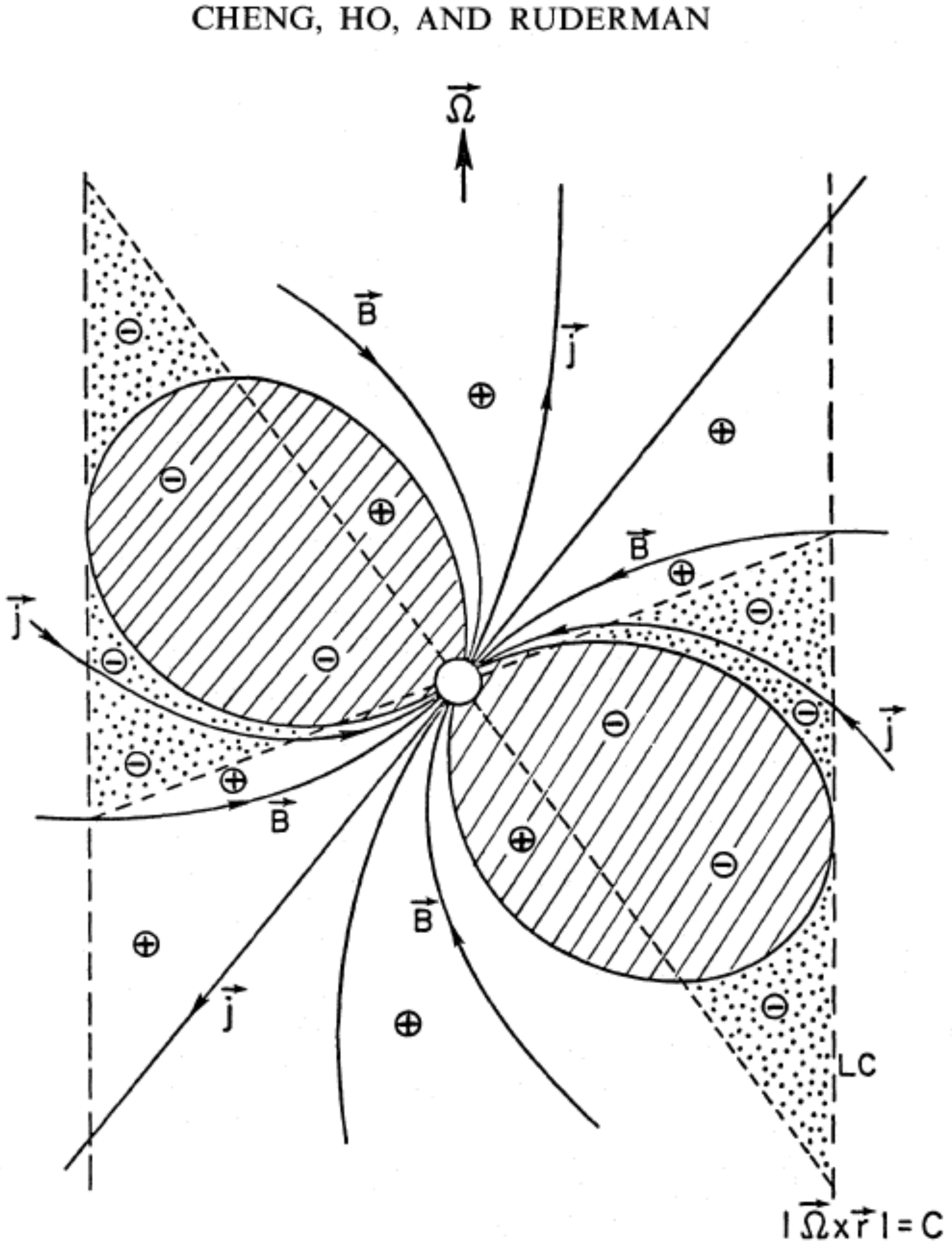

- Stellar rotation tends to generate an electric field,

$$\vec{E} = -\frac{1}{c}\left(\vec{\Omega} \times \vec{r}\right) \times \vec{B}$$

- The maximum voltage drop (vacuum)

$$\Delta\Phi \approx \frac{\Omega^2 B_\star R_\star^3}{2c^2} \approx \pi \left(\frac{3I}{2c}\frac{\dot{P}}{P^3}\right)^{1/2} \simeq 2.2 \times 10^{15}\ \text{Volts}$$

- At the stellar surface, $\vec{E} \cdot \vec{B} \neq 0$, so particles flow out of the star to cancel the electric field, creating the magnetosphere, bounded by the light cylinder.
- Acceleration models assume available a fraction of ΔΦ.
- Acceleration scenarios are based on acceleration at polar caps or outer gaps $\rho = \vec{\Omega} \cdot \vec{B}/2\pi c = 0$
- Relativistic particles leave the magnetosphere through open field lines inducing a pulsar wind.

Hester et al. (2002)

Chandra

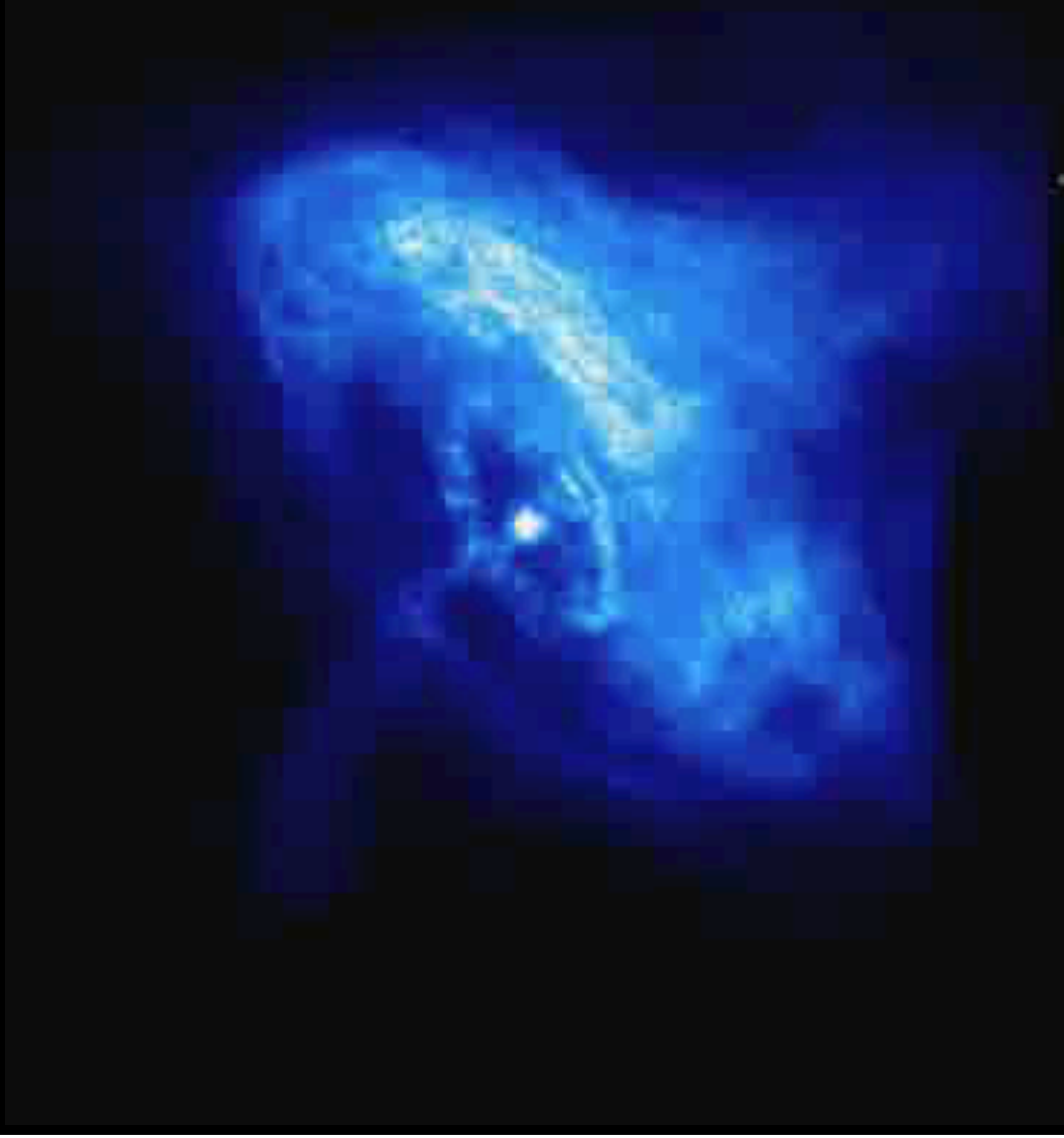

HST

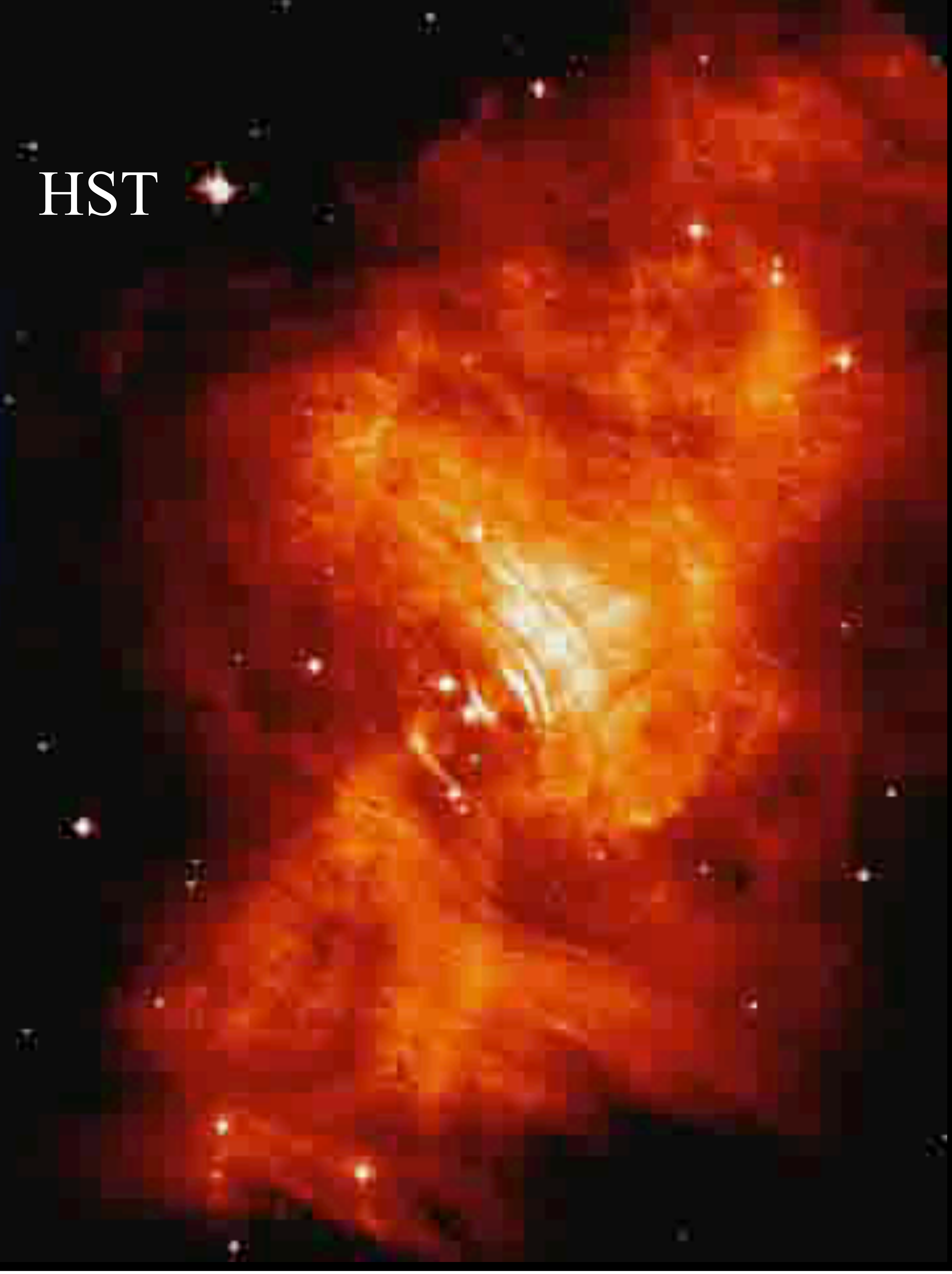

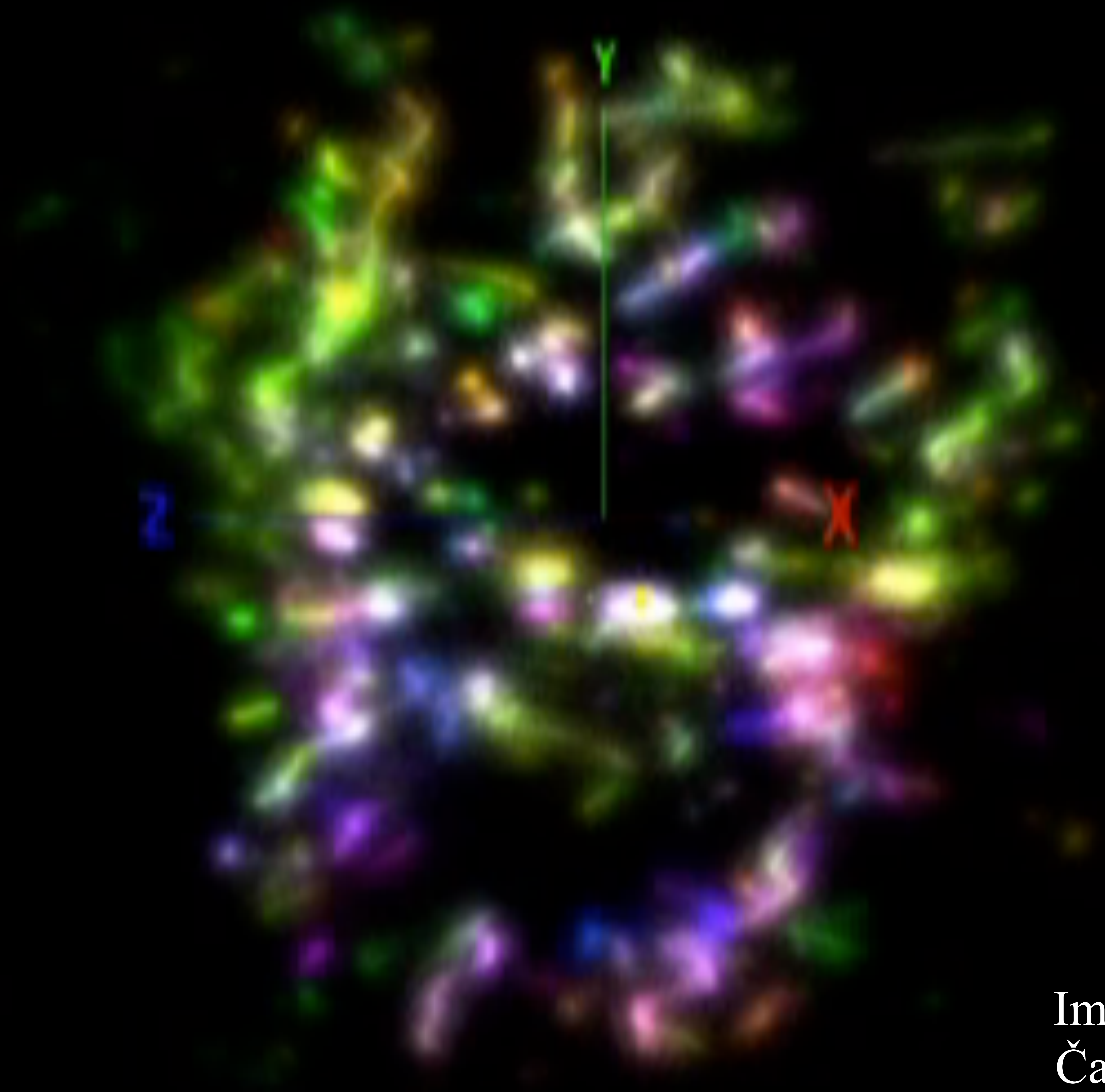

Imaging of M1 @ OAGH, Cananea
Čadež, Carramiñana & Vidrih 2004

Evolution

- The evolution of the environment plays a role in the diffusion of electrons.
- The evolution of the pulsar plays a role in supplying the electrons.

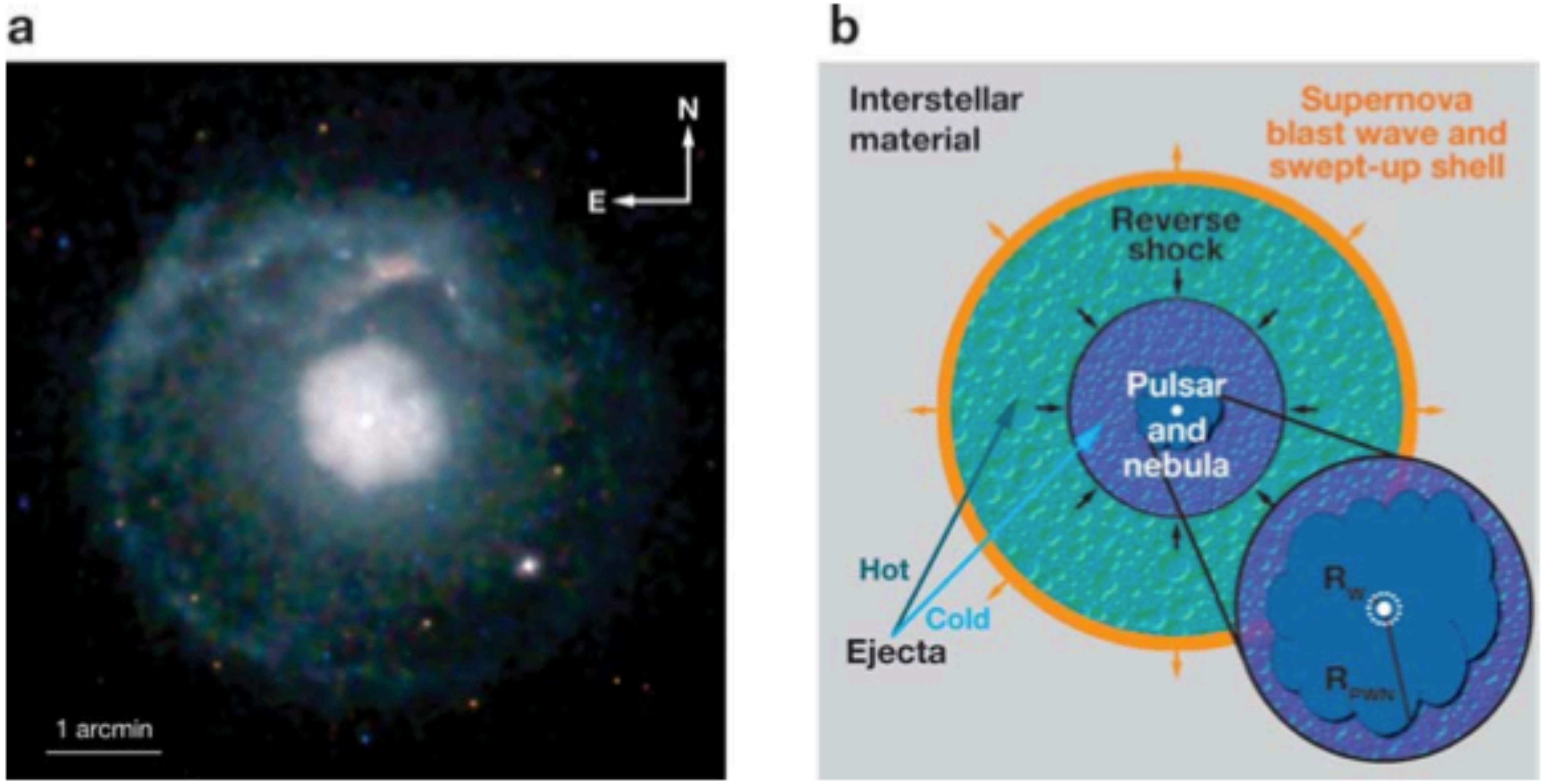

Figure 2

(*a*) A deep *Chandra* X-ray image of the composite SNR G21.5–0.9 (Matheson & Safi-Harb 2005). A circular supernova remnant (SNR) of diameter ≈5′ surrounds a symmetric pulsar wind nebula (PWN) of diameter ≈1′.5, with the young pulsar J1833-1034 at the center (Gutpa et al., 2005; Camilo et al., 2006). The central location of the pulsar and PWN and the symmetric appearance of the PWN and SNR both argue for a relatively unevolved system in which the PWN expands freely and symmetrically into the unshocked interior of the SNR. (*b*) A schematic diagram of a composite SNR showing the swept-up interstellar medium shell, hot and cold ejecta separated by the reverse shock, and the central pulsar and its nebula. The expanded PWN view shows the wind termination shock. Note that this diagram does not correspond directly to G21.5–0.9, in that a significant reverse shock has probably yet to form in this young SNR.

Gaensler & Slane (2006)

Pulsar evolution

- Estimates of energy released in e^+e^- depend on pulsar spin-down history.
- Magnetic dipole model predicts, $n = \frac{\ddot{\Omega}\Omega}{\dot{\Omega}^2} = 3 + 2\left(\frac{\dot{B}_\star/B_\star}{\dot{\Omega}/\Omega}\right)$ inconsistent with observed n < 3.
- Pulsar evolution is highly dependent on the model.
- In Alvarez & Carramiñana (2004) we considered the effect of a monopolar term.

To be continued!

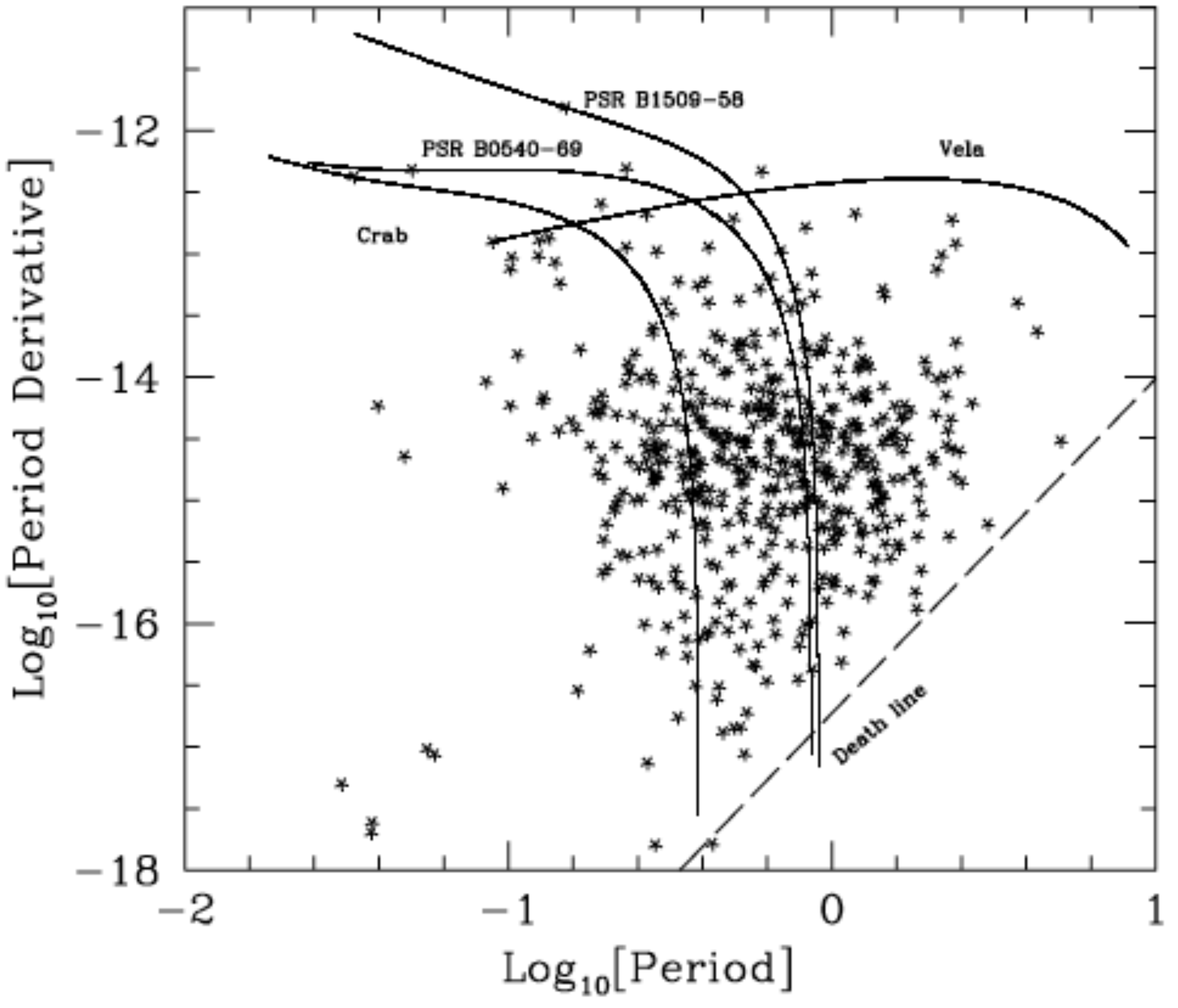

Fig. 8. Evolutionary trajectories for the Crab, PSR B1509–58, PSR B0540–69 and Vela, using an inverse linear decay-law for the magnetic field. The decay timescale used is $t_c = 10^4$ except for Vela where $t_c = 1.04\times10^5$ years. The trajectories were run for $10^3\ t_c$, except that of Vela which was run for $10t_c$.